

RESEARCH

Open Access

Tylophorine, a phenanthraindolizidine alkaloid isolated from *Tylophora indica* exerts antiangiogenic and antitumor activity by targeting vascular endothelial growth factor receptor 2-mediated angiogenesis

Sarita Saraswati^{1*}, Pawan K Kanaujia², Shakti Kumar³, Ranjeet Kumar⁴ and Abdulqader A Alhaider⁵

Abstract

Background: Anti-angiogenesis targeting VEGFR2 has been considered as an important strategy for cancer therapy. Tylophorine is known to possess anti-inflammatory and antitumor activity, but its roles in tumor angiogenesis, the key step involved in tumor growth and metastasis, and the involved molecular mechanism is still unknown. Therefore, we examined its anti-angiogenic effects and mechanisms *in vitro* and *in vivo*.

Methods: We used tylophorine and analyzed its inhibitory effects on human umbilical vein endothelial cells (HUVEC) *in vitro* and Ehrlich ascites carcinoma (EAC) tumor *in vivo*.

Results: Tylophorine significantly inhibited a series of VEGF-induced angiogenesis processes including proliferation, migration, and tube formation of endothelial cells. Besides, it directly inhibited VEGFR2 tyrosine kinase activity and its downstream signaling pathways including Akt, Erk and ROS in endothelial cells. Using HUVECs we demonstrated that tylophorine inhibited VEGF-stimulated inflammatory responses including IL-6, IL-8, TNF- α , IFN- γ , MMP-2 and NO secretion. Tylophorine significantly inhibited neovascularization in sponge implant angiogenesis assay and also inhibited tumor angiogenesis and tumor growth *in vivo*. Molecular docking simulation indicated that tylophorine could form hydrogen bonds and aromatic interactions within the ATP-binding region of the VEGFR2 kinase unit.

Conclusion: Tylophorine exerts anti-angiogenesis effects via VEGFR2 signaling pathway thus, may be a viable drug candidate in anti-angiogenesis and anti-cancer therapies.

Keywords: Tylophorine, VEGFR2, Antiangiogenesis, Microvessel density, Molecular docking

Background

Angiogenesis, the formation of new blood vessels by sprouting from pre-existing endothelium [1], one of the characteristic of malignant neoplasia development [2]. Angiogenesis blockade has been shown to be an effective strategy in inhibiting tumor growth and metastasis [3]. A major pro-angiogenic cytokine is vascular endothelial growth factor (VEGF) which comprises several isoforms, including VEGF-A (vascular permeability factor), VEGF-B,

VEGF-C and VEGF-D, as numerous splice variant isoforms [4]. VEGF exerts its biological actions on the endothelial cells is mediated by two types of receptor tyrosine kinases (RTKs), namely VEGFR1 (Flt-1) and VEGFR2 (KDR/ Flk-1) with high affinities [4]. VEGFR2 plays an important role in mediating the mitogenesis and permeability of endothelial cells. Autophosphorylation of Tyr¹¹⁷⁵ on VEGFR2 is crucial for endothelial cell proliferation, and leads to the activation of downstream signaling events including Src family kinase [5], focal adhesion kinase (FAK) [6,7], phosphoinositide 3 kinase/AKT kinase, Mammalian target of rapamycin (mTOR) [8], protein kinase C/protein kinase D, mitogen extracellular kinase/ extracellular

* Correspondence: saritasaraswati@gmail.com

¹Camel Biomedical Research Unit, College of Pharmacy and Medicine, King Saud University, Riyadh, Kingdom of Saudi Arabia
Full list of author information is available at the end of the article

signal related kinase (ERK) that subsequently promote proliferation, migration, and tube formation of endothelial cells in pre-existing vasculature. Recently many studies showed the important role of VEGFR2 in potential drug discovery and molecular mechanism research [9]. Considering anti-angiogenesis therapy is to target endothelial cells that support tumor growth rather than cancer cells themselves, VEGFR2 has become an important therapeutic target for cancer anti-angiogenesis therapy [10-13].

The National Institutes of Health (NIH) website provides a basic summary of anti-angiogenic drugs that were or are still currently under clinical investigations (<http://www.cancer.gov/clinicaltrials/developments/antiangio-table>). These include monoclonal antibodies targeting VEGF ligands or VEGFRs [14], soluble receptors that sequester ligands [15] and small molecule inhibitors that inhibit kinase activity [16]. Three drugs developed for their anti-angiogenic actions, bevacizumab (Avastin[®]), sunitinib malate (Sutent[®], SU11248) and sorafenib (Nexavar[®], BAY 43-9006), have been approved by the United States Food and Drug Administration for treatment of patients with specific types of cancer—all three inhibit VEGF signaling by blocking VEGF ligand or VEGFR [17]. However, serious side effects, such as hypertension, bleeding and gastrointestinal perforation, have been associated with currently available anti-VEGF agents, limiting their chronic use [17]. Hence, there is an urgent need to find a molecule that can be more specific and less toxic for the treatment of cancer, particularly agents that exhibit activity against drug-resistant strains, completely sterilize the infection, or shorten the duration of drug therapy and thus promote drug compliance.

Tylophorine (Figure 1A) and its analogs are phenanthroindolizidine alkaloids, isolated from *Tylophora indica* (Asclepiadaceae) [18]. *Tylophora indica* has been included as an official drug in the Bengal pharmacopoeia of 1884 [19]. The leaves of this plant have been used for the treatment of asthma as well as bronchitis, rheumatism and dysentery in India. These alkaloids possess anticancer [20-24], anti-inflammatory [19,25], anti-ameobical [26] and anti-viral [27] activity. Several key metabolic enzymes, including thymidylate synthase [28] and dihydrofolate reductase have been reported as biological targets of tylophorine alkaloids [29]. Tylophorine derivatives also inhibit activator protein-1-mediated, CRE-mediated, and nuclear factor kappaB (NF- κ B)-mediated transcription [30,31]. Tylophorine arrests the cells at G1 phase in HepG2, HONE-1, and NUGC-3 carcinoma cells and down regulates cyclin A2 expression [32]. Preliminary studies illustrate the potential of tylophorine as a new class of anticancer drugs. However, the molecular mechanism responsible of its inhibitory effects on cancer cell growth is largely unknown. In this study, we evaluated for the first time how tylophorine inhibits tumor angiogenesis by targeting key signaling pathways on human endothelial cells

and *in vivo* mouse model. Our results demonstrate that tylophorine significantly inhibited VEGF-stimulated endothelial cell proliferation, migration and tube formation *in vitro*. Tylophorine inhibited neovascularization in sponge implant angiogenesis assay *in vivo* and further attenuated tumor associated angiogenesis. Furthermore, mechanistically, tylophorine suppressed VEGFR2-mediated signaling pathway. Meanwhile, the structure-based interaction between tylophorine and VEGFR2 was found to be stable conformation based on *in-silico* analysis which revealed that hydrogen bond and aromatic interactions were formed. Taken together our results suggest that tylophorine could be used as a potential anti-angiogenesis agent that targets VEGF/VEGFR2 signaling pathways and inhibits tumor induced angiogenesis.

Results

Tylophorine inhibited cell viability in endothelial cells

Angiogenesis is primarily initiated by growth factors therefore we tested whether tylophorine decreases VEGF-mediated HUVEC viability and proliferation. We found that when HUVECs were cultured in normal cell culture medium (ECGM supplemented with 20% FBS) in absence of VEGF, tylophorine inhibited cell viability in a dose- and time-dependent manner. Significant cell viability inhibitory effect of tylophorine was observed in HUVECs at concentrations more than 10 μ M (Figure 1B). As shown in Figure 1C, the proliferation of endothelial cells stimulated by VEGF was markedly decreased after tylophorine treatment ranging from 2.5 to 20 μ M at different time intervals of 24 and 48 h indicating extracellular VEGF acted as a strong attractant for endothelial cells proliferation. Tylophorine alone inhibited the growth of HUVEC in dose dependent manner (Additional file 1: Figure S1A). As detected by BrdU incorporation assay (Figure 1D), DNA synthesis of HUVECs was also significantly inhibited by tylophorine in a dose-dependent manner. To further examine whether tylophorine would result in toxic effects of HUVEC, LDH cytotoxic assay was carried out. As shown in Figure 1E, Tylophorine caused minute toxicity on HUVECs.

Tylophorine inhibited VEGF-induced endothelial cell migration and invasion and tube formation of HUVECs

Cell migration is an essential step in angiogenesis [33]; therefore we investigated the effects of tylophorine on the chemotactic motility of the endothelial cells by using wound-healing (Figure 2A) assay. The results showed that tylophorine significantly inhibited VEGF-induced HUVECs migration in a dose-dependent manner ranging from 2.5 μ M to 20 μ M. Directional motility and matrix degradation are crucial for angiogenesis sprouting therefore, we next examined the effect of tylophorine on the invasion ability of HUVECs using the Boyden

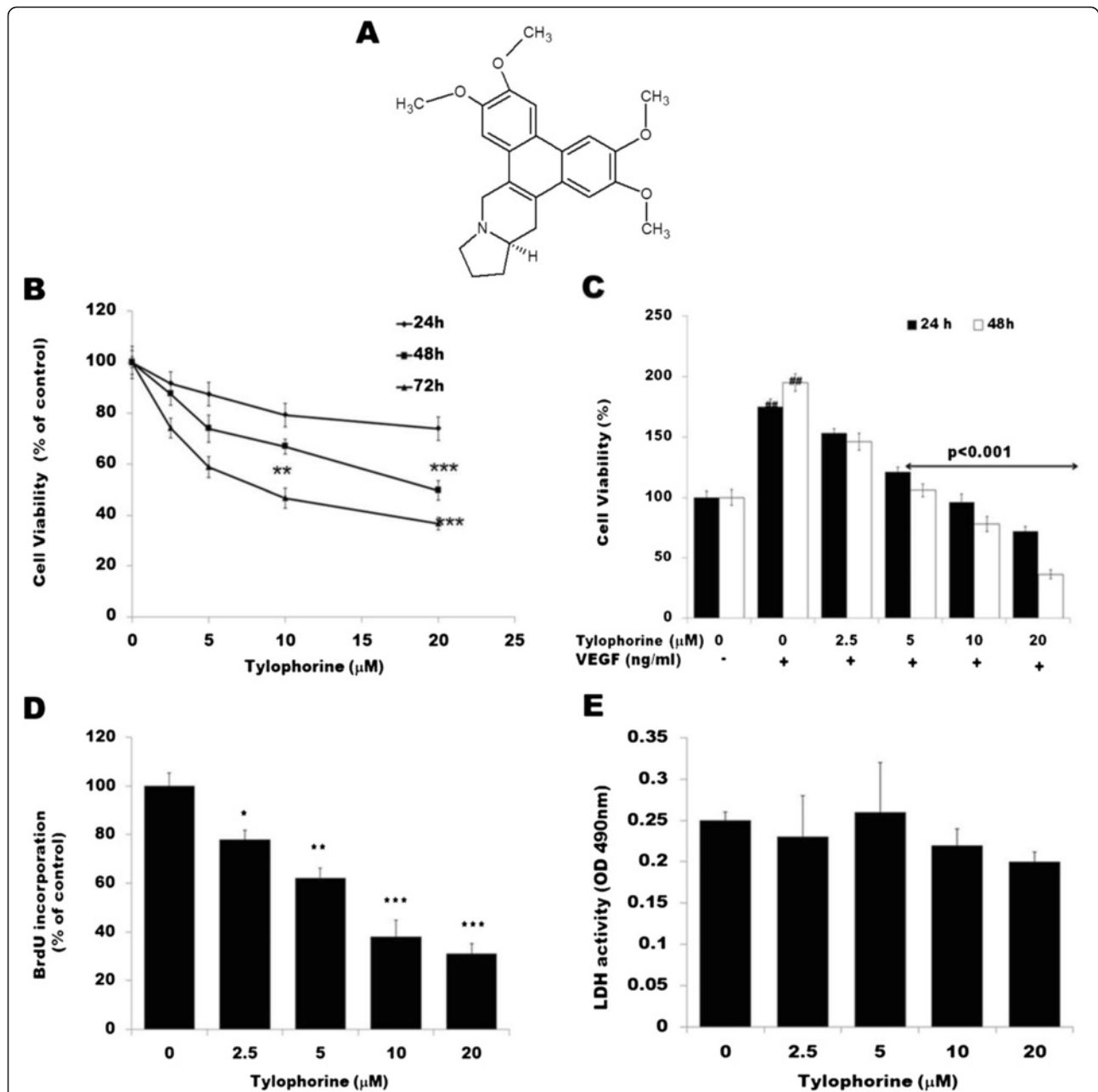
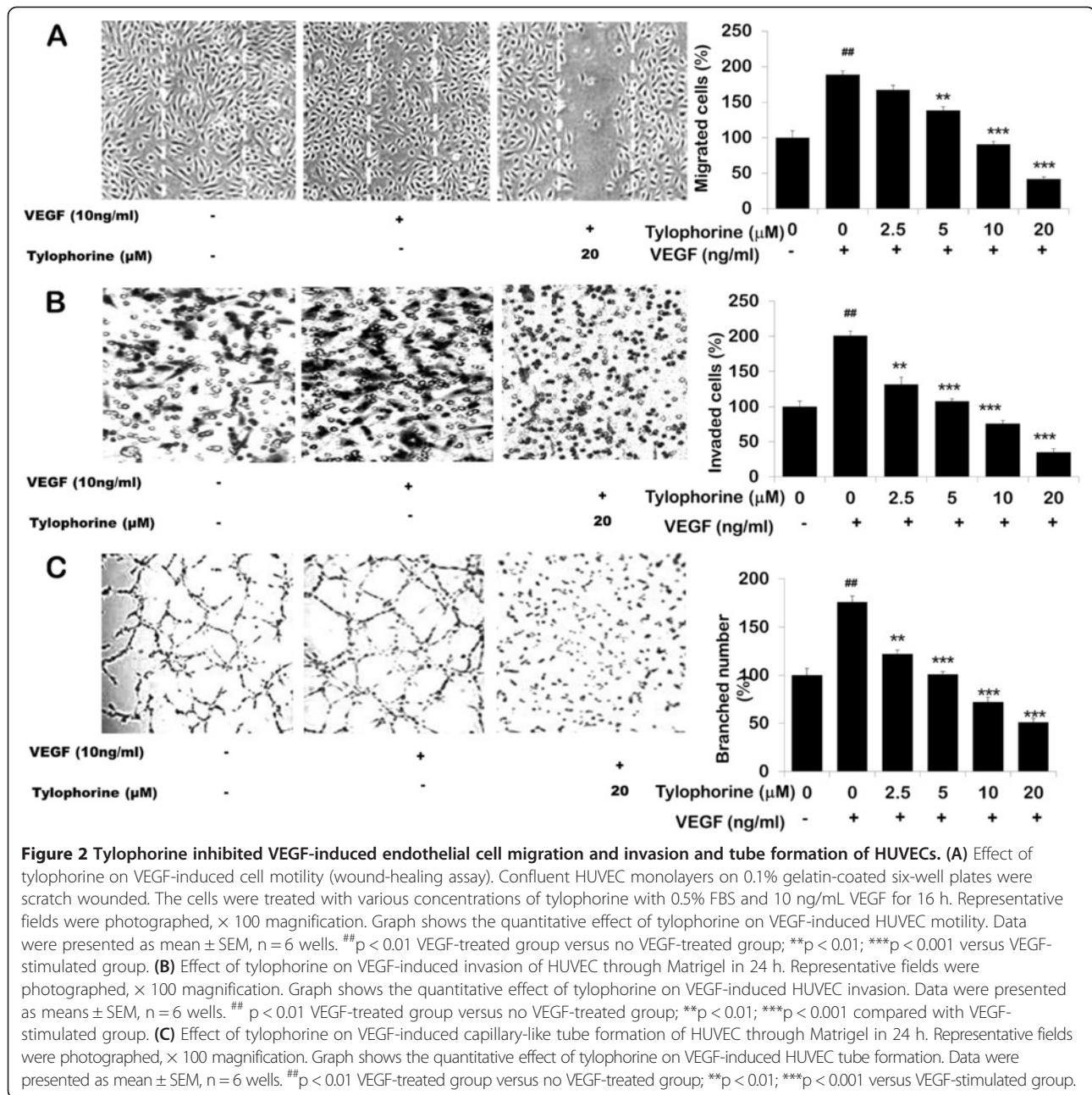


Figure 1 Effect of tylophorine on cell proliferation in HUVECs. (A) Chemical structure **(B)** Under normal culture condition. HUVECs were cultured in ECGM containing 20% FBS, then cells (5×10^4 cells/well) were treated with DMSO (0.1%) or various concentrations of tylophorine for 24, 48 and 72 h. Cell viability was determined by MTT assay. Cells receiving only DMSO (0.1%) served as a vehicle control. Data were expressed as percentages of the vehicle control (100%) as mean \pm SEM, n = 6 wells. **p < 0.01; ***p < 0.001 versus control group. **(C)** Under VEGF-stimulated condition HUVECs (5×10^4 cells/well) were starved with ECGM supplemented with 0.5% FBS for 24 h, and then treated with or without VEGF (10 ng/ml) and DMSO (0.1%) or various concentrations of tylophorine for another 24 and 48 h. Data were expressed as percentages of the vehicle control (100%) as mean \pm SEM, n = 6 wells. **(D)** Effects of tylophorine on DNA synthesis was examined by BrdU cell proliferation enzyme linked immunosorbent assay. Data were expressed as percentages of the vehicle control (100%) as mean \pm SEM, n = 6 wells. *p < 0.05; **p < 0.01; ***p < 0.001 versus control group. **(E)** Tylophorine administration did not result in LDH release from endothelial cells as studied with LDH cytotoxicity assay kit indicating that tylophorine posed little cytotoxicity effects upon HUVECs. Data were expressed as percentages of the vehicle control (100%) as mean \pm SEM, n = 6 wells.

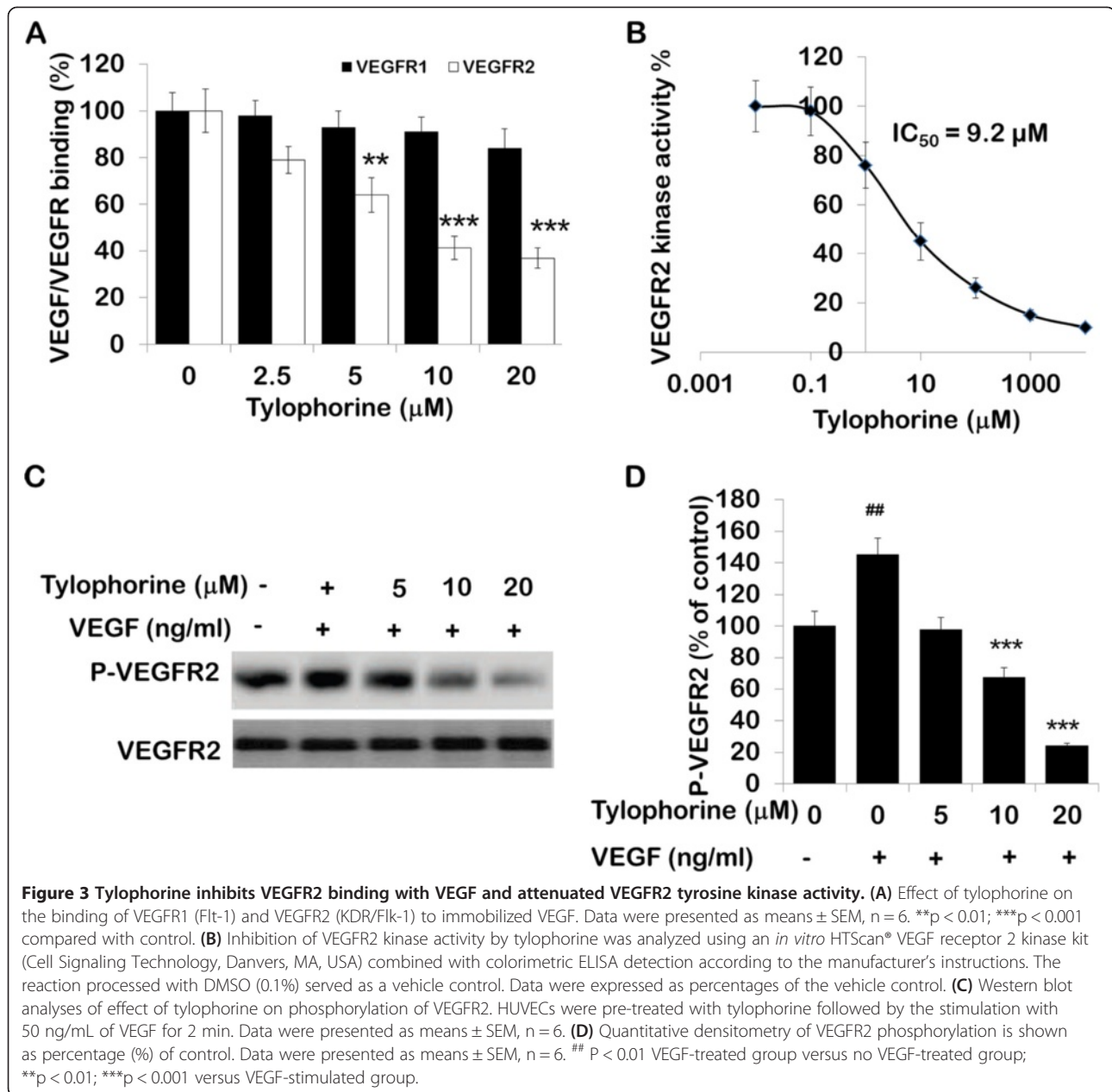


chamber assay. As shown in Figure 2B, a large number of cells migrated to the lower side of membrane in the transwell chamber after stimulation with VEGF. However, the number of invaded cells were significantly low in the presence of tylophorine ($p < 0.001$). The maturation of migrated endothelial cells into a capillary tube is a critical step during angiogenesis [34]. Thus, we investigated its effect on HUVEC tube formation. When HUVECs were seeded on the growth factor-reduced matrigel, robust tubular-like structures were formed in the presence of VEGF (Figure 2C). Almost 80% destruction of tube network was observed when HUVECs were

incubated with tylophorine at 10 μ M ($p < 0.001$). Taken together, tylophorine suppressed VEGF-induced angiogenesis *in vitro* by inhibiting the migration, invasion and tubular structure formation of endothelial cells.

Differential effect of tylophorine on the binding of VEGF to its receptors

Further, we investigated whether tylophorine inhibits the binding of VEGF to its receptors, VEGFR1 (Flt-1) and VEGFR2 (Flk-1/KDR). As shown in Figure 3A, tylophorine decreased the binding of VEGFR2 to immobilized VEGF with IC_{50} of $\sim 12.29 \mu$ M. However,



tylophorine did affected the binding between VEGF and VEGFR1 (Figure 3A) but it did not reached to significant level. Antihuman VEGFR1 antibody (AF321, R&D Systems) and antihuman VEGFR2 antibody (MAB3572, R&D Systems) were used as positive control for VEGFR1 and VEGFR2 respectively (data not shown).

Tylophorine attenuated VEGFR2 tyrosine kinase activity

Previous studies suggested that blockage of VEGFR-2 activity could significantly limit tumoral neovascularization process [12]. Therefore, we first investigated whether tylophorine decreased P-VEGFR2 levels by inhibiting the kinase activity of VEGFR2 using an ELISA-based

tyrosine kinase assay. Tylophorine was found to inhibit kinase activity of VEGFR2 (Figure 3B) with an IC_{50} of $\sim 9.2 \mu M$. SU5416, a known inhibitor of VEGFR2, was used as a positive control and showed inhibition of kinase activity with an IC_{50} of $1.5 \mu M$ (data not shown), as described previously [35].

We further examined the effects of tylophorine on phosphorylation of VEGFR2 to determine its inhibitory effect on VEGFR2-mediated signaling pathways in endothelial cells. We found that VEGFR2 was phosphorylated by the addition of exogenous VEGF to HUVECs (Figure 3C). Pretreatment of cells with tylophorine significantly blocked VEGF-induced phosphorylation of

VEGFR2, without affecting overall VEGFR2 expression levels. Quantitative densitometry of protein phosphorylation is shown as percentage (%) of vehicle control (Figure 3D). The protein levels were normalized to β -actin. In addition, previous studies supported that phosphorylation of VEGFR2 could subsequently trigger multiple downstream signals that induced proliferation and differentiation activities of endothelial cells [36,37].

Tylophorine inhibited the activation of VEGFR2-mediated signaling pathways

Binding of VEGFR2 with VEGF led to the activation of various downstream signaling molecules responsible for endothelial cell migration, proliferation and survival [35]. To further delineate the mechanism that underlies the anti-angiogenic effects of tylophorine, we screened some key kinases involved in VEGFR2-mediated signaling pathway. VEGF induces survival of endothelial cells (ECs) mainly via the activation of AKT [37], whereas activation of ERK1/2 MAPKs is thought to be essential for VEGF-induced proliferation [38]. To assess the effect of tylophorine on these pathways, serum-starved HUVECs were treated with VEGF for 20 minutes in the presence or absence of tylophorine and cell lysates were subjected to immunodetection using antibodies against

either P-AKT (Ser⁴⁷³) or P-ERK1/2. The result showed that P-ERK1/2 is enhanced by VEGF treatment while the expression level of ERK1/2 remains unchanged. Tylophorine was found to inhibit the phosphorylation of ERK1/2 at the concentration of 20 μ M without affecting total ERK1/2 expression level (Figure 4A). A recent study suggests that the AKT/mTOR pathways and Hsp90, which are critical for angiogenesis, are phosphorylated or activated by VEGFR2 activation in the endothelial cells [39]. As shown in Figure 4A, expression levels of P-AKT and p-mTOR increases by VEGF treatment. Pretreatment of the HUVECs with tylophorine significantly inhibited the phosphorylation of AKT and mTOR, while the total amount of AKT and mTOR remains unchanged. Further, the action of tylophorine on the phosphorylation of FAK and Src were determined. The result showed that tylophorine inhibited VEGF-induced phosphorylation of FAK at the dose of 10 and 20 μ M and Src at the concentration of 20 μ M respectively (Figure 4A). Tylophorine could evidently inhibit VEGF-stimulated eNOS expression. In addition, both the MMP-9 and MMP-2 activities were suppressed with tylophorine treatment (Figure 4B). ROS is known to be downstream signaling after VEGFR2 activation [40], therefore, we detected the ROS levels by DCFH-DA

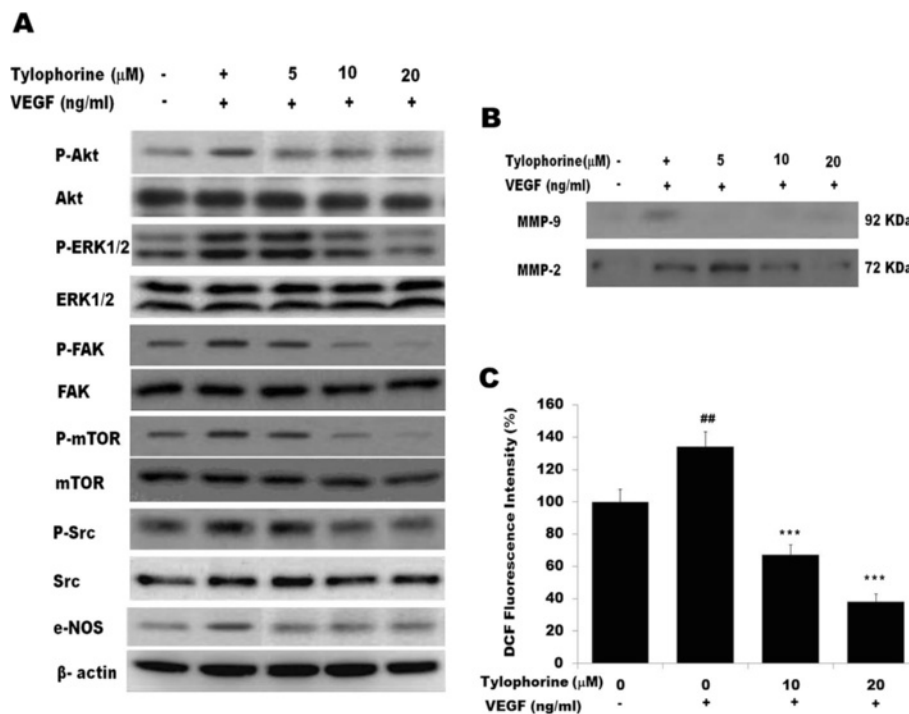


Figure 4 Western blot analysis of the effect of tylophorine on VEGFR2-mediated downstream signaling. **(A)** HUVECs were pre-treated with tylophorine followed by the stimulation with 50 ng/mL of VEGF for 20 min. Data were presented as means \pm SEM, n = 6. **(B)** Effect of tylophorine on VEGF-induced MMP-2 secretion from HUVECs after 20 h examined by zymography. Data were presented as means \pm SEM, n = 6. **(C)** Effect of tylophorine on HUVECs intracellular ROS level as detected by DCFH-DA staining assay. Data were presented as means \pm SEM, n = 6. ^{##}p < 0.01 VEGF-treated group versus no VEGF-treated group; ^{**}p < 0.01; ^{***}p < 0.001 versus VEGF-stimulated group.

probe. The results showed that the intracellular ROS levels were significantly reduced after tylophorine administration (Figure 4C). Taken together, our result revealed that tylophorine inhibited *in vitro* angiogenesis by directly targeting VEGFR2 on the surface of endothelial cells, and further downregulating VEGFR2-mediated signaling pathway.

Tylophorine inhibited VEGF-induced IL-6, IL-8, TNF- α , IFN- γ , MMP-2 and NO

During inflammation VEGFR activation is linked to cytokine release, pro-inflammatory molecules and leukocyte endothelial interactions, which exacerbate the inflammatory response [41]. Therefore, we investigated the effect tylophorine on endothelial cell cytokine release. As shown in Figure 5, HUVECs treated for 24 h with VEGF up-regulated the secretion of IL-6 (Figure 5A), IL-8 (Figure 5B), TNF- α (Figure 5C), IFN- γ (Figure 5D) and MMP-2 (Figure 5E). HUVECs pretreated with tylophorine, before the addition of VEGF (10 ng/mL), significantly ($P < 0.001$) decreased the cytokine secretion IL-6, IL-8, TNF- α , IFN- γ and MMP-2 in a dose-dependent manner (Figure 5). Further tylophorine significantly inhibited NO levels (Figure 5F, $P < 0.001$) in HUVEC at 24 h incubation in a dose-dependent manner.

Tylophorine inhibited neovascularization in vivo

To determine whether tylophorine has an effect on angiogenesis *in vivo*, we performed a sponge implant angiogenesis assay in Swiss albino mice. Sponge disks were *s.c.* implanted into mice and treatment with tylophorine or DMSO was continued, once daily, for 14 days. Over 14 day experimental period, the weight of sponge granuloma tissues increased gradually in vehicle-control group, whereas in tylophorine treated group sponge weight was reduced dramatically (Figure 6A). Daily administration of tylophorine into the sponge implants caused a marked decrease in angiogenesis as evident by pictorial representation (Figure 6B) and decreased hemoglobin concentration (Figure 6C) in sponge granuloma tissues. In implants of control group, the hemoglobin levels were found to be $3.11 \pm 0.17 \mu\text{g Hb/mg}$ wet tissue ($n = 10$); versus $2.21 \pm 0.52 \mu\text{g Hb/mg}$ (tylophorine 7.5 mg/kg; $n = 10$) and $1.24 \pm 0.19 \mu\text{g Hb/mg}$ wet tissue (tylophorine 15 mg/kg; $n = 10$). The difference in between control and treated groups were further confirmed by morphometric analysis of implants that the number of blood vessels was markedly lower in the treated groups as compared to control group (Figure 6D), which was confirmed by staining with CD31. It was observed that tylophorine treatment significantly reduced

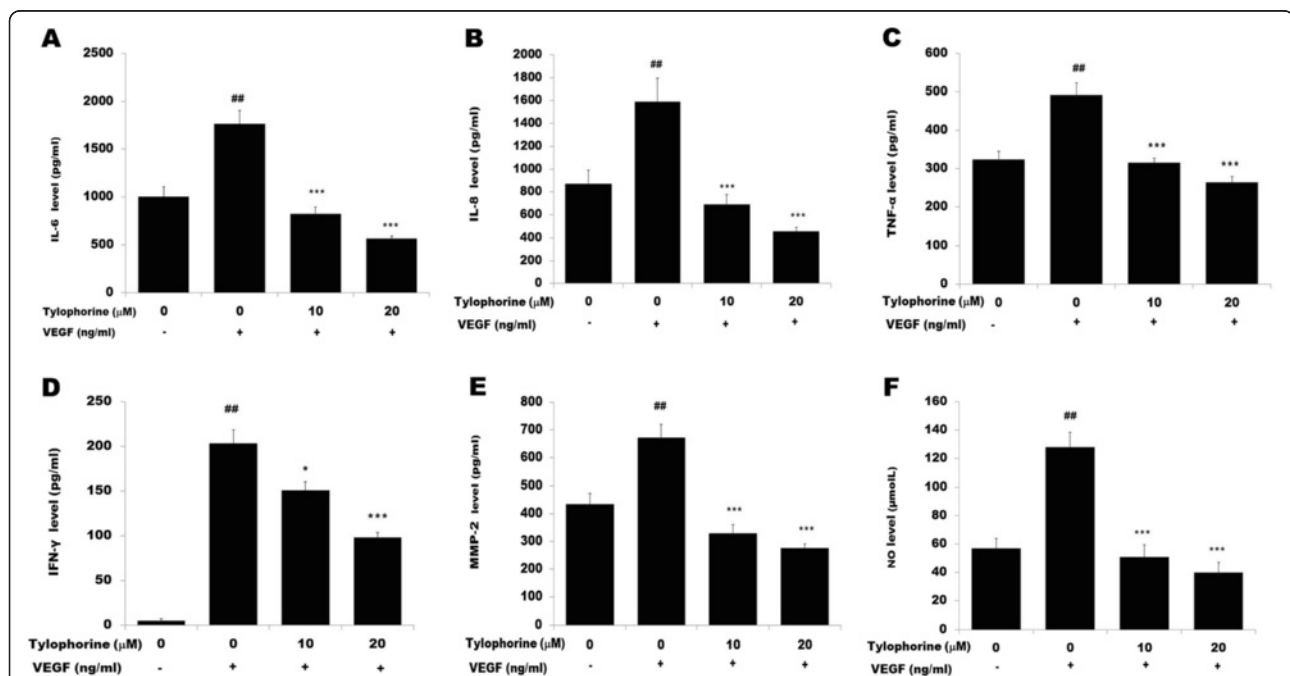
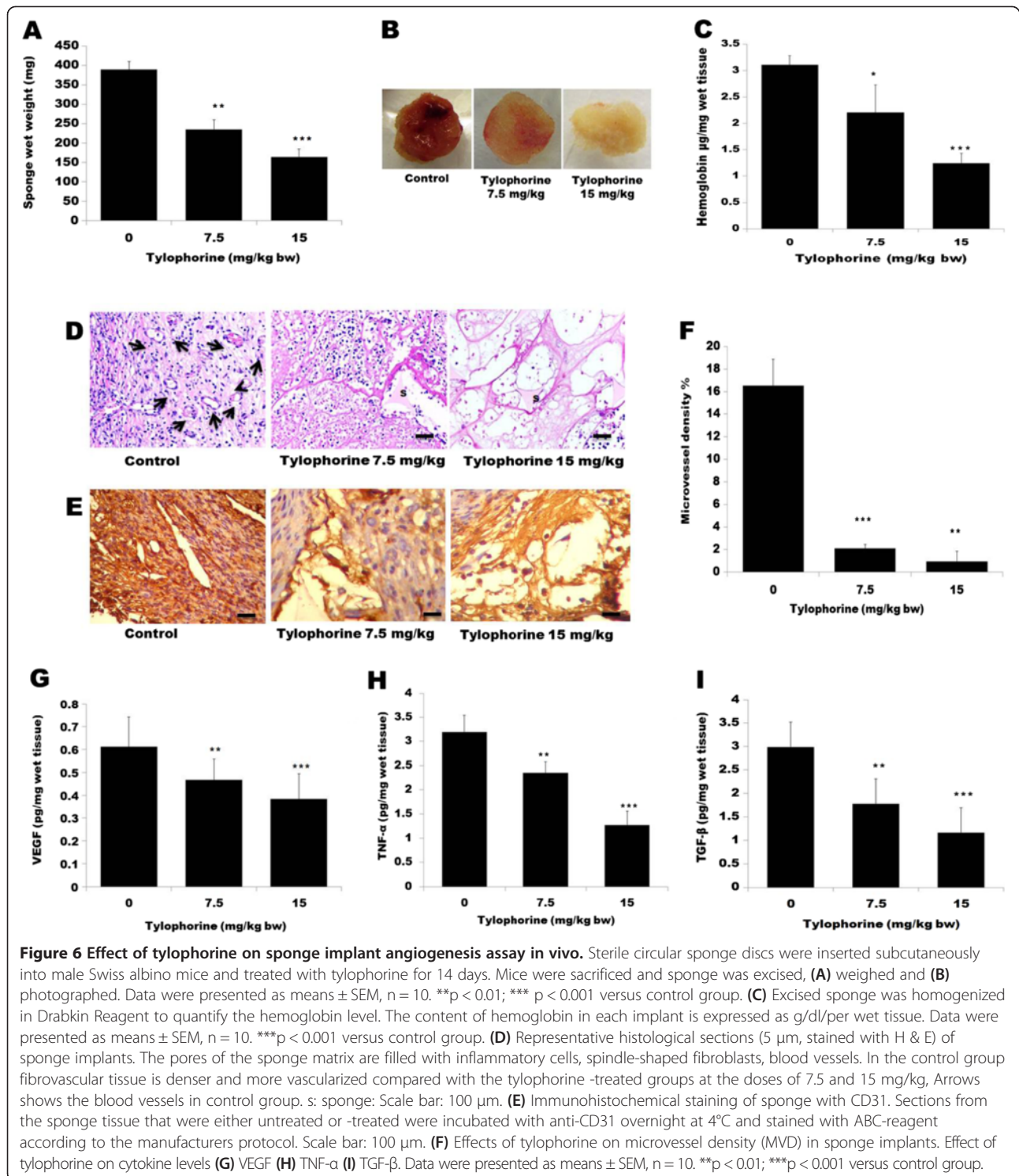


Figure 5 Effect of tylophorine on secretion of VEGF-induced cytokines. (A) IL-6, (B) IL-8, (C) TNF- α (D) IFN- γ (E) MMP-2 and (F) NO.

Serum-starved HUVECs were preincubated with DMSO (0.1%) or tylophorine (20 μM), before stimulation with VEGF (10 ng/mL), and supernatants were harvested after 24 h for cytokine assays. IL-6, IL-8, TNF- α , IFN- γ and MMP-2 were measured by sandwich ELISA following the manufacturer's instructions (R and D systems, USA). Absorbance was determined using a microplate reader (Biorad, USA) at 450 nm. The NO levels in the HUVECs were measured with Nitric oxide colorimetric assay kit (Biovision, USA) following the manufacturer's instructions. Absorbance was determined using a microplate reader (Biorad, USA) at 540 nm. Data were presented as means \pm SEM, $n = 3$. # $p < 0.01$ VEGF-treated group versus no VEGF-treated group; ** $p < 0.01$; *** $p < 0.001$ versus VEGF-stimulated group.



the CD 31 expression as compared to control group (Figure 6E). The microvessel density was statistically lowered in tylophorine treated sponge tissue (Figure 6F). Subsequently, it was sought to correlate this change in vascularization with change in the level of VEGF in the implants. It was found that tylophorine significantly

inhibited VEGF level in sponge implant tissues (Figure 6G). The inflammatory components of the sponge-induced inflammation were determined by estimating the numbers of the leukocytes in the implant by assaying levels of pro-inflammatory cytokines TNF- α . Tylophorine at 15 mg/kg reduced the TNF- α level by 41.81% (Figure 6H). As shown

in Figure 6I, there was a clear decrease in the TGF- β levels (38.92 and 59.73% at 7.5 and 15 mg/kg respectively) after tylophorine treatment.

Tylophorine inhibited tumor growth *in vivo*

Prompted by the *in vitro* and *in vivo* data supporting a potential antiangiogenic activity of tylophorine, we examined the *in vivo* efficacy of tylophorine on the growth of mouse Ehrlich ascites solid tumor, which is highly dependent on angiogenesis. As compared to control group treated with vehicle, tylophorine -treated group showed slower growth kinetics of EAC solid tumor (Figure 7A). It was found that treatment with tylophorine significantly led to suppression of EAC solid tumor volumes when compared with the control group. The average tumor volume in the control group increases from $91.35 \pm 21.64 \text{ mm}^3$ to $2139.05 \pm 193.09 \text{ mm}^3$ after 30 days, whereas the average tumor volume in the tylophorine-treated mice increased from $93.28 \pm 31.98 \text{ mm}^3$ to $213.96 \pm 65.61 \text{ mm}^3$ (Figure 7A). The body weights of animals corresponded well with the growth of tumors in respective group of animals (Figure 7B). The effect of tylophorine alone on body weight of normal mice is depicted in Additional file 2:

Figure S2. Quantitatively weights of tumor lumps treated with tylophorine were also found smaller ($p < 0.001$) as compared to control group (Figure 7C). The average tumor weight in the control group was $8.34 \pm 1.85 \text{ g}$; whereas the average tumor weight in the tylophorine -treated group was found to be $0.98 \pm 0.07 \text{ g}$ (Figure 7D) indicating that proliferation rate of tumor cells in mice was greatly inhibited by tylophorine. To further examine whether tylophorine could suppress tumor growth by inhibiting angiogenesis, tumor tissues were stained with specific antibodies against CD31, P-VEGFR2 (Tyr 1175), P-AKT, and P-Erk in Figure 7E. CD31 is a widely used endothelial marker for quantifying angiogenesis by calculating microvessel density (MVD) [42]. Our data showed that the average number of blood vessels in tylophorine treated group is 4.87 ± 0.34 blood vessels/HPF (Figure 7F) as compared with 11.93 ± 2.84 blood vessels/HPF in the control group ($P < 0.001$). Suppressed CD31 expression and decreased tumor volume and tumor weight suggests that tylophorine targets endothelial cells (ECs) as well as tumor cells. In addition, tylophorine down-regulated the expressions of P-VEGFR2, P-Akt, and P-Erk (Figure 7E) further demonstrating that tylophorine played an important

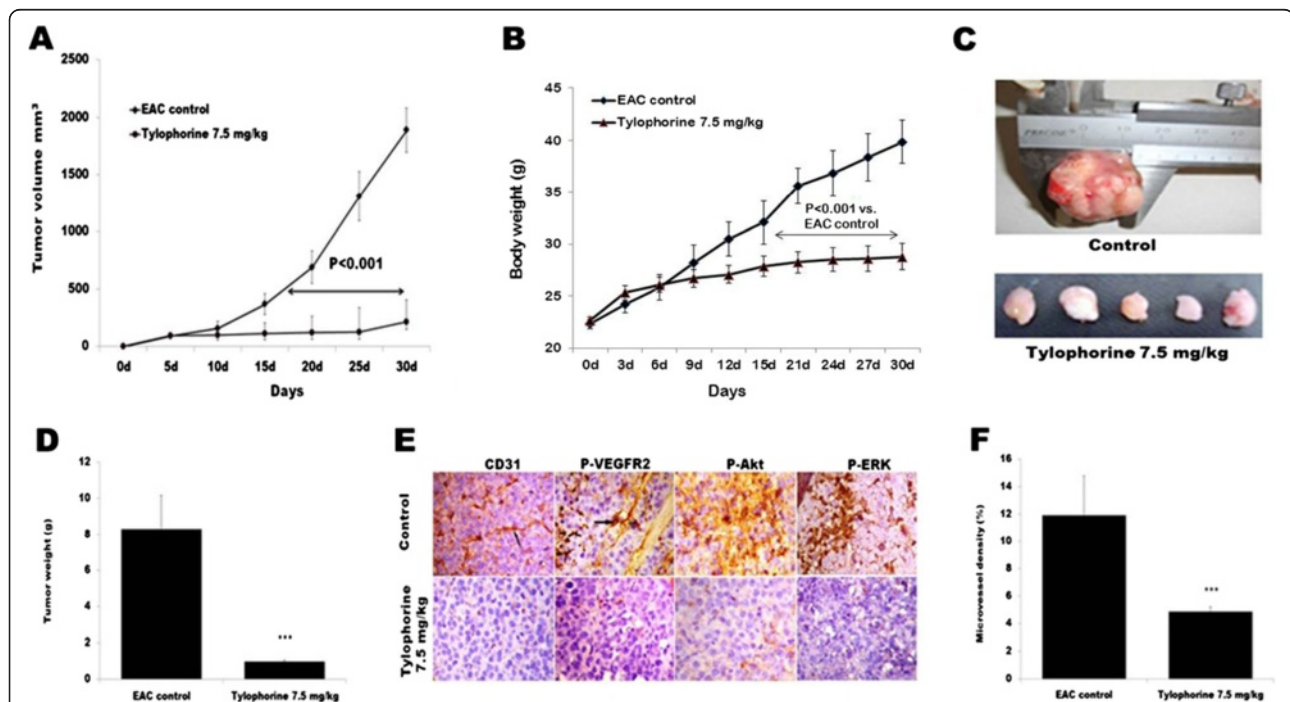


Figure 7 Effect of tylophorine on tumor growth and VEGFR2 phosphorylation in EAC tumor model. 15×10^6 EAC cells/mouse were injected s.c. into 5–6 week old Swiss albino mice. After solid tumors grew to $\sim 100 \text{ mm}^3$, the mice were *i.p.* treated with tylophorine (7.5 mg/kg bw). Tumor growth was measured with calipers every fifth days using the formula: $\text{Tumor volume}(\text{mm}^3) = (\text{width})^2 \times (\text{length}) \times \pi/6$. Tylophorine treatment decreases (A) tumor volume (B) body weight. Data were presented as means \pm SEM, $n = 15$. (C) Representative images of solid tumor lump shows tylophorine treated group is significantly smaller than those in the control group. (D) The tumor tissue was removed from mice at 30 days after treatment and weighed. (E) Immunohistochemical staining of tumor tissue ($n = 6$) with antibodies against P-VEGFR2, P-ERK, P-Akt and CD31. (F) % MVD was determined by selecting the blood vessel (CD31) area per field in selected vascularized areas divided by the whole area. Data were presented as means \pm SEM, $n = 6$. *** $p < 0.001$ versus control group.

role in suppressing angiogenesis at least partly through VEGFR2 signaling pathways.

Tylophorine prolongs the survival of tumor bearing mice

The tumor bearing mice administered with DMSO or tylophorine (7.5 mg/kg bw) for 30 days were observed and the days of survival were recorded. With tylophorine treatment, the survival of tumor bearing mice significantly increased from 35.2 ± 1.29 days to 70.3 ± 3.28 days (Figure 8) as obtained by Kaplan Meier's survival analysis (Figure 8).

Tylophorine located at the ATP-binding sites of VEGFR2 kinase domain

We next analyzed the binding pattern between tylophorine and VEGFR2 kinase domain to further understand how tylophorine exerted anti-angiogenesis effects via VEGFR2 and its signaling pathways. When molecular docking simulation between tylophorine ligand and VEGFR2 protein was analyzed, it was found that tylophorine has bound at slightly different location toward N-terminal domain from original bound ligand 42Q with -7.00 Kcal/mol binding affinity in the ATP binding pocket (Figure 9A). There are five amino acids *i.e.*, Lys868, Leu870, His879, Leu882 and Leu912 are actively involved in the binding of tylophorine. His879 is an active amino acid of the ATP binding pocket has participated in hydrogen bond with tylophorine. Rest amino acids are hydrophobic in nature and have made strong π - π bonds with the ligand. Therefore hydrophobic interaction is more dominant than hydrogen and electrostatic interaction in tylophorine-VEGFR2 complex (Figure 9B). When structure of tylophorine was inspected, it has found that its core structure has made up with three fused benzene rings which are also hydrophobic nature suggesting, it may be reason for dominancy of hydrophobic interaction. Such binding pattern of tylophorine within VEGFR2 may prohibit the binding of the ATP at its binding

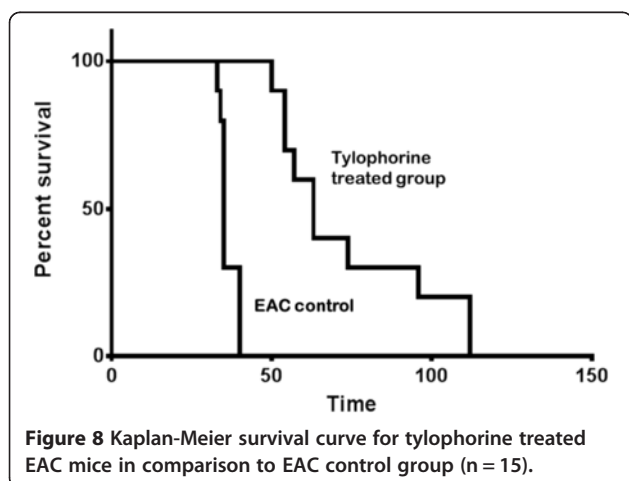
pocket and in this way it has provided a direction for development of small natural inhibitors.

Discussion

The present study demonstrated that tylophorine exhibited anti-angiogenic activities *in vivo* and suppressed key steps involved in angiogenesis including proliferation (Figure 1C), migration (Figure 2A), invasion (Figure 2B), tubulogenesis (Figure 2C) and expression of pro-MMP2 (Figure 4B) as detected by gelatin zymography in endothelial cells. By directly blocking VEGFR2 phosphorylation and activation, tylophorine inhibited VEGFR2 kinase activity (Figure 3B) as well as suppressed VEGFR2 signaling pathway (Figure 4A) *in vitro*. Supporting evidences concerning *in vivo* anti-angiogenesis effects of tylophorine then came from sponge implant angiogenesis model and Ehrlich ascites carcinoma tumor model. Tylophorine significantly inhibited blood vessels formation in sponge implant assay (Figure 6) and significantly suppressed tumor growth accompanied by reduction in microvessel density (MVD) in tumor tissues (Figure 7).

Our study provides a novel and mechanistic insights into the mechanism by which tylophorine affects the multiple facets of vascular endothelial angiogenic signaling through VEGFR1 and VEGFR2. Phosphorylated Tyr1175 of VEGFR2 mediates activation of the mitogen-activated protein kinase/ERK cascade and was shown to contribute to cell proliferation in endothelial cells [38-40]. Src family kinase is substantially involved in VEGF-induced angiogenesis *in vitro* and *in vivo* [43-45]. Other signaling molecules that have been involved in VEGF-induced migration through VEGFR2 include FAK and its substrate paxillin, which are participated in focal adhesion during cell migration [6,46]. By interacting between FAK and Src, a dual kinase complex FAK-Src forms, and is activated by multiple integrin-regulated linkages [47]. Recent studies show that inhibition of ERK, phosphoinositide 3-kinase, PDK1/Akt and FAK downstream of VEGFR2 has emerged as a target for anticancer therapy [48]. AKT/mTOR/ribosomal protein S6 kinase (p70S6K) signaling has also been identified as a novel, functional mediator in angiogenesis [48,49]. VEGFR1 plays a positive role in promoting tumor angiogenesis by cross-talks among epithelial cells and other cell types because VEGFR1 is expressed not only endothelial cells but also on macrophage lineage cells and tumor epithelial cells [50]. VEGFR1 is a kinase-impaired RTK, and may signal in the context of a receptor heterodimer [51].

Our studies indicated that tylophorine interfered with the binding of VEGFR2 and reduced the autophosphorylation of VEGFR2 whereas; tylophorine did not affect the VEGF binding to VEGFR1. We also found that a half-maximum inhibitory concentration 9.2 μ M



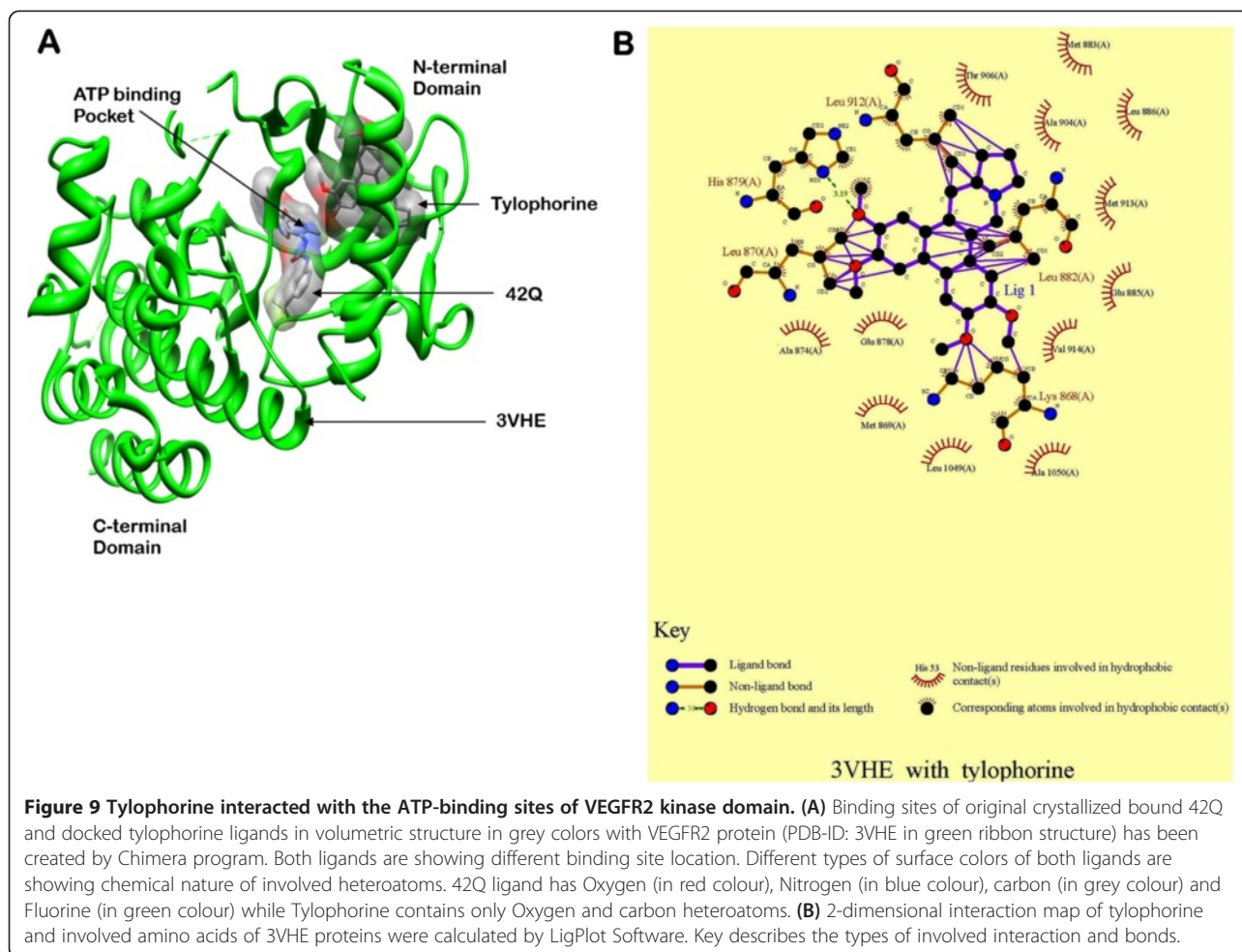


(Figure 3B) of tylophorine significantly blocked the kinase activity of VEGFR2. Further it was observed that tylophorine modulates VEGF-mediated vascular permeability and angiogenesis by inhibiting phosphorylation of Akt, ERK, FAK, mTOR, Src and eNOS (Figure 3C) in endothelial cells *in vitro*. In addition, it was also found that tylophorine inhibited MMPs activity in a dose-dependent manner, suggesting that decreased MMPs activity might be also responsible for interfering with the binding of VEGF to VEGFR2, and thus inhibiting the neo-angiogenesis process [52]. Furthermore, ROS was reported as a downstream signaling of VEGFR2 and served as a survival mediator in supporting endothelial cell proliferation [53]. Our results demonstrated that the ROS level decreased significantly after tylophorine administration, which might be a consequence event of decreased VEGFR2 activity. All these results suggested that tylophorine inhibits the VEGFR2 signaling pathways.

As mentioned above, dimerization within the extracellular domain of VEGFR2 could induce the autophosphorylation on numerous tyrosine residues within its intracellular domain. The phosphorylation is an ATP

consuming process. The ATP-binding region lies between N-terminal lobe and C-terminal lobe within VEGFR2 catalytic domain. Many kinase inhibitors could exert their inhibitory effects through purely or partially competing against the adenosine triphosphate (ATP) and subsequently suppressing the receptor autophosphorylation. They were acting as ATP mimetics that bound to this site and competed with cellular ATP [33]. In this study, tylophorine could stably locate at the ATP-binding pocket near the hinge region. There are five amino acids i.e., Lys868, Leu870, His879, Leu882 and Leu912 at the ATP pocket were essential for the stable conformation of VEGFR2/tylophorine complex. Rest amino acids are hydrophobic in nature and have made strong π - π bonds with the ligand. All the unique binding modes largely promoted the conformational stability of the tylophorine/VEGFR2 complex.

Conclusion

Overall our study indicated that tylophorine exerted potent anti-angiogenesis activities via specifically targeting VEGFR2 and its signaling pathway. As a natural

inhibitor against VEGFR2, tylophorine is a promising candidate for development of anti-angiogenesis agents.

Methods

Chemicals and reagents

Tylophorine was purchased from Enzo Life Sciences (UK) Ltd. Phosphate-buffered saline (PBS), Tween 20, fetal bovine serum (FBS), bovine serum albumin (BSA), phenylmethanesulfonyl fluoride (PMSF), ethylenediaminetetraacetic acid (EDTA), heparin, HEPES buffer, penicillin, streptomycin, NaHCO₃, amphotericin B, dimethyl sulfoxide (DMSO) and gelatin were obtained from Sigma (St. Louis, MO, USA). Tylophorine was dissolved in 0.1% DMSO to form a 100 mM solution, stored at -20°C in small aliquots until needed and protected from light, and then diluted to various concentrations as needed. Growth factor-reduced Matrigel was purchased from BD Biosciences (San Diego, CA). The antibodies anti-β-actin, anti-VEGFR2, anti-Src, anti-FAK, anti-ERK1/2, anti-AKT, anti-mTOR, anti-CD31, phospho-specific anti-VEGFR2 (Tyr¹¹⁷⁵), anti-c-Src (Tyr⁴¹⁶), anti-FAK (Tyr^{576/577}), anti-ERK1/2 (Thr²⁰²/Tyr²⁰⁴), anti-AKT (Ser⁴⁷³), anti-mTOR (Ser²⁴⁴⁸), Phototope® HRP Western blotting detection System (LumiGLO® chemiluminescent reagent and peroxide), TMB substrate and stop solution were delivered from Cell Signaling Technology (Danvers, MA, USA). VEGF, IL-6, IL-8, TNF-α, and IFN-γ were procured from R and D systems (MN, USA). M199 medium and sodium dodecyl sulfate polyacrylamide electrophoresis (SDS-PAGE) gels were acquired from Invitrogen (Life Technologies, Grand Island, NY, USA).

Cell lines and cell culture

Human umbilical vascular endothelial cells (HUVECs) (Clonetics, Lonza, Basel, Switzerland) were cultured in endothelial cell growth medium (ECGM): M199 medium supplemented with 20% FBS, 20 μM bECGF, 0.1 mg/mL heparin, 15 mM HEPES buffer, 50 IU/L penicillin, 50 mg/L streptomycin, 44 mM NaHCO₃, and 50 μg/mL amphotericin B under a humidified chamber at 37°C with 5% CO₂.

Cell viability assay

HUVECs (5 × 10⁴ cells/well) were plated onto a gelatinized 24-well culture plate and cultured in ECGM containing 20% FBS. HUVECs were treated with DMSO (0.1%) or different concentrations of tylophorine (0, 2.5, 5, 10, 20 μM) for 24, 48 and 72 h. Cell viability was determined by MTT assay as described previously [54]. After 4 h of incubation, the absorbance was measured at 450 nm with a microplate reader (Biorad, USA). The results were calculated from six replicates of each experiment. Three independent experiments were performed.

Next, we determined the effects of tylophorine on VEGF-induced cell viability. HUVECs (5 × 10⁴ cells/well) were starved with ECGM containing 0.5% FBS for 24 h. After the pre-incubation, cells were treated with or without VEGF (10 ng/mL) and DMSO (0.1%) or different concentrations of tylophorine and incubated for another 24 and 48 h. Cell viability was quantified by MTT assay. The group without VEGF and tylophorine treatment was set as 100%. The results were the means calculated from six replicates of each experiment. Three independent experiments were performed.

BrdU incorporation assay

DNA synthesis was determined by bromodeoxyuridine (BrdU) labeling assay using Cell Proliferation ELISA, BrdU (colorimetric) kit. In brief, 5 × 10⁴ HUVECs per well (100 μl in ECGM + 20% FBS) were seeded in a gelatin coated for overnight attachment. Then the cultivated medium was replaced with serum-free medium supplemented with 10 ng/mL VEGF as well as different concentrations of tylophorine in a final volume of 100 μl / well. After 24 h, cells were labeled with BrdU (2 h, 37°C, 4 h), incubated with Fix Denat solution (30 min, 20°C), and reincubated with Anti-BrdU POD (90 min, 20°C). The absorbance was read at 450 nm in a microplate reader (Biorad, USA). The assay was repeated three times independently.

Lactate dehydrogenase (LDH) toxicity assay

The LDH release assay was performed using a cytotoxicity detection kit plus (LDH) (Roche Diagnostics) according to the manufacturer's instructions. In brief, HUVECs were seeded in 96-well plate at a density of 5 × 10⁴ cells per well. After incubation with various concentrations of tylophorine for 24 h, cell supernatants were collected and analyzed. The absorbance of formed formazan was read at 490 nm on a microplate reader (Biorad, USA). The LDH content of each sample was calculated according to the following formula: Cytotoxicity(%) = [(experimental value - low control)/(high control - low control)] × 100. The assay was repeated three times independently.

Endothelial cell migration assay: wound healing

HUVECs (5 × 10⁴ cells/well) were allowed to grow to full confluence in 6-well plates pre-coated with 0.1% gelatin and then starved with ECGM containing 0.5% FBS for 6 h to inactivate cell proliferation. After that, cells were wounded with pipette tips and washed with PBS. ECGM supplemented with 0.5% FBS was added into the wells with or without VEGF (10 ng/mL) and DMSO (0.1%) or different concentration of tylophorine. Images of cells were taken using an inverted microscope (Eclipse TS100, Nikon, Japan) at 100 × magnification after 16 h of

incubation in a humidified atmosphere with 5% CO₂ at 37°C. The migrated cells were observed from three randomly selected fields and quantified by manual counting. Cells receiving only DMSO served as a vehicle control. Inhibition percentage was expressed as percentage of the vehicle control (100%). The assay was repeated three times independently.

Endothelial cell invasion assay

Cell invasion assay was performed using Transwell chambers with 6.5 mm diameter polycarbonate membrane (8-μm-sized pores). Upper surfaces of transwell inserts were coated with matrigel. The bottom chamber of the apparatus contained 600 μL of endothelial cell medium supplemented with 10 ng/mL VEGF or tylophorine at different concentrations. The HUVECs (100 μL) were added to the upper chamber (5 × 10⁴ cells/well) and incubated in endothelial cell medium. After 24 h incubation at 37°C, non-invasive cells on the upper membrane surfaces were removed by wiping with cotton swabs. Cell invasion was quantified by counting cells on the lower surface using phase contrast microscope (Eclipse TS100, Nikon, Japan) at 100 × magnification. The results were the means calculated from three replicates of each experiment. The assay was repeated three times independently.

Endothelial cell capillary-like tube formation assay

Matrigel™ basement membrane matrix (growth factor reduced) (BD Biosciences, San Jose, CA, USA) was thawed at 4°C, pipetted into pre-chilled 24-well plates (100 μL matrigel/well) and incubated at 37°C for 45 min. HUVECs were firstly incubated in ECGM supplemented with 0.5% FBS for 10 h and then treated with DMSO (0.1%) or different concentrations of tylophorine for 30 min before seeding. Cells were collected and placed onto the layer of matrigel (5 × 10⁴ cells/well) in 1 mL of ECGM supplemented with 0.5% FBS, followed by the addition of VEGF (10 ng/mL). After 24 h of incubation with 5% CO₂ at 37°C, the network-like structures of endothelial cells were examined under an inverted microscope (Eclipse TS100, Nikon, Japan) at 100 × magnifications. Branching points in three random fields per well was quantified by manual counting. Cells receiving only DMSO (0.1%) served as a vehicle control. Inhibition percentage was expressed as percentage of the vehicle control (100%). The assay was repeated three times independently.

VEGFR binding assay

VEGFR binding assay was performed as described previously [55]. Briefly, VEGF (50 ng/mL) in 50 μL of PBS were immobilized to 96-well plates. The wells were washed and blocked with 3% bovine serum albumin

(BSA) in PBS for 2 h. Tylophorine with 1% BSA in PBS were added with VEGFR1 (Flt-/Fc, 20 ng/mL; R&D Systems, Minneapolis, MN) or VEGFR2 (KDR/Flk-1; 20 ng/mL; R&D Systems, Minneapolis, MN) to VEGF-coated wells. After 3 h incubation, the wells were washed thrice with PBST. Flt-1 or KDR/Flk-1 bound to VEGF was determined by biotinylated anti-human IgG (Dako) and horseradish peroxidase-conjugated streptavidin (Sigma), developed with tetramethylbenzidine substrate reagent (BD Biosciences), and quantified by measuring the absorbance at 450 nm.

In vitro VEGFR2 kinase inhibition assay

In vitro VEGFR2 tyrosine kinase activity was assayed using HTScan® VEGFR2 kinase assay kit (Cell Signaling Technology, USA) combined with colorimetric ELISA detection as described previously [56]. The final reaction system included 60 mmol/L HEPES (pH 7.5), 5 mmol/L MgCl₂, 5 mmol/L MnCl₂, 3 μmol/L Na₃VO₄, 1.25 mmol/L DTT, 20 μmol/L ATP, 1.5 μmol/L substrate peptide, 100 ng of VEGF receptor kinase and indicated concentrations of tylophorine. The results were expressed as percent kinase activity of the vehicle control (100%), and IC₅₀ was defined as the compound concentration that resulted in 50% inhibition of enzyme activity. The kinase assay was performed thrice independently.

Western blotting analysis

In brief, cell lysates (50 μg) were separated by 8% SDS PAGE and transferred to polyvinylidene difluoride membranes. Membranes were then incubated with primary antibodies including phosphorylated and/or total VEGFR2, ERK1/2, AKT, mTOR, c-Src, FAK, eNOS and β-actin (Cell Signaling Technology, USA). After overnight incubation at 4°C, membranes were washed with TBST three times and then incubated with secondary antibodies at room temperature for 2 h. Immunoreactive bands were then visualized by the enhanced chemiluminescence (ECL) detection system (GE healthcare). Cells receiving only DMSO (0.1%) served as a vehicle control. Three independent experiments were performed in triplicates.

Gelatin zymography

HUVECs (80% confluent) were washed with serum-free M199 and incubated with or without VEGF (10 ng/mL) containing tylophorine for 20 h. The proteins in conditioned medium were size fractionated on a 10% SDS-polyacrylamide gel impregnated with 0.1% gelatin. MMP2 and other MMPs were activated in gel for 18 h at 37°C. Gels were fixed, stained with 0.25% Coomassie brilliant blue R250, and destained. Gelatinase activity was visualized as cleared band on the stained gel.

Measurement of reactive oxygen species

2',7'-Dichlorofluorescein diacetate (DCFH-DA, Sigma, St. Louis, MO) was used to measure ROS formation. After exposed to different concentrations of tylophorine for 24 h, endothelial cells were then incubated in 10 μ M DCFH-DA at 37°C for 20 min. Cells were washed with PBS three times to remove DCFH-DA that not entered in cells. The fluorescence of oxidized probe was measured using a microplate reader (Synergy Mx Multimode, Biotek, US). The fluorescence was visualized immediately at wave lengths of 485 nm for excitation and 530 nm for emission by inverted fluorescence microscope. Total green fluorescence intensities of each well were quantified using image analysis software.

Cytokine immunoassays

Secreted IL-6, IL-8, TNF- α , IFN- γ and MMP-2 levels in tylophorine treated HUVEC culture medium were measured using an ELISA kit (R and D Systems, MN, USA) according to manufacturer's instructions.

Nitric oxide (NO) measurement

Secreted NO level in tylophorine treated HUVEC culture medium were measured using a Nitric oxide colorimetric assay kit (Biovision, USA) according to manufacturer's instructions.

Sponge implant angiogenesis assay

Sponge implant assay was performed as described previously [57,58]. Sterile circular sponge discs were inserted subcutaneously into male Swiss albino mice (n = 10). The day of sponge insertion was taken as day 0. Commencing day 1, animals were treated with tylophorine (7.5 and 15 mg/kg bw) from day 1 to day 14. On the day following the last injection (day 15) mice were sacrificed and the sponges were excised, weighed and photographed. Sponges were bisected; one half was fixed in 10% formalin and embedded in paraffin wax. Sections (5 μ m) were stained with hematoxylin/eosin for identification of blood vessels. The second half of the sponge was weighed, homogenized in 2 mL of sterile PBS at 4°C, and centrifuged (2000 \times g for 30 min) to quantify level of VEGF, TNF- α and TGF- β . The extent of the vascularization of the sponge implants was assessed by the amount of hemoglobin (Hb) detected in the tissue using the Drabkin method [59]. All procedures for animal experimentation used were approved by the Institutional Animal Ethics Committee.

In vivo antitumor activity

Ehrlich ascites carcinoma (EAC) cells (15×10^6) were implanted subcutaneously into female Swiss albino mice, 5-6 weeks old, weighing 20-25 g [60,61]. After tumors became palpable, the mice were divided into two groups

(n = 15 each) based on the tumor size of each mouse so that the average tumor volume was equal between the groups. One group of mice (n = 15) was injected with vehicle (0.1% DMSO) and the other group (n = 15) were injected with 7.5 mg/kg bw tylophorine, intraperitoneally (*i.p.*), every day. The tumor volume was measured using a vernier caliper and calculated according to the modified ellipsoid formula: Tumor volume(mm^3) = (width)² \times (length) \times $\pi/6$. The effect of tylophorine on percentage increase in life span was calculated on the basis of mortality of the experimental mice (n = 15) in solid tumor [33]. For determination of mean survival time (MST) and percentage increased life span (% ILS), animals were allowed to natural death [38]. After 30 days of treatment, the mice were sacrificed and whole tumor tissues were excised, weighed and photographed. Excised tumors were fixed in 10% formaldehyde and embedded in paraffin. 5- μ m sections were stained with hematoxylin and eosin (H & E) and immunostained with antibodies against mouse CD31 (Santa Cruz biotechnology, UK), VEGF, P-ERK, P-Akt, and P-VEGFR2 (Cell Signaling, USA), and visualized by appropriate biotin-conjugated secondary antibodies followed by immunoperoxidase detection with the Vectastain ABC Elite kit (Linaris, Germany) and diaminobenzidine (DAB) substrate (Vector, UK). Counterstaining was performed with hematoxylin. Microvessel density was calculated using Image J software (NIH, Bethesda, MD) [28,33]. All procedures for animal experimentation used were approved by the Institutional Animal Ethics Committee.

Molecular docking

Computational based study of molecular interaction between tylophorine and VEGFR2 receptor was carried out using Autodock Vina software [62]. Ligand structures were optimized by using MarvinSketch program. Protein and ligand were prepared for docking simulation by adding of Gasteiger partial charges [63] and polar hydrogen with the help of AutoDock Tool program. X-ray crystal structures of VEGFR2 protein (PDB-ID: 3VHE) with small molecule, 42Q was downloaded from Protein Data Bank (<http://www.rcsb.org>). Water molecules and other heteroatom were manually removed out from the protein structures. 3D structure of tylophorine ligand was downloaded from PubChem database (www.ncbi.nlm.nih.gov/PubChem). A grid cube box with 60 \AA \times 60 \AA \times 60 \AA dimension was centered on the originally crystallized 42Q ligand for searching the most suitable binding site of tylophorine during molecular docking simulation and exhaustiveness option was set up at 8. Chimera (www.cgl.ucsf.edu/chimera) and LigPlot [64] programs were used to analyze and visualizing the molecular interaction between the ligand and receptor with default parameter.

Statistical analysis

The data were analyzed using SigmaStat 3.5 software. Results were presented as the mean \pm S.E. from at least three independent experiments. One-way analysis of variance (ANOVA) was followed by the Newman-Keuls test, when appropriate, to determine the statistical significance of the difference between means. The Mann–Whitney *U* test was used to compare microvessel density in different tumor samples. A *p* value of < 0.05 was considered statistically significant.

Additional files

Additional file 1: Figure S1. Effect of tylophorine on growth inhibition in HUVECs.

Additional file 2: Figure S2. Effect of tylophorine on body weight in normal mice treated with tylophorine at 7.5 mg/kg.

Competing interest

The authors' declared that they have no competing interest.

Authors' contributions

SS designed study; acquired, analyzed and interpreted data; performed statistical analysis and drafted and revised the manuscript. PKK participated in acquisition of data, statistical analysis and manuscript preparation. SK, RK and AAA participated in experimental data acquisition and revision of manuscript. All authors read and approved the final version of manuscript.

Acknowledgement

The authors especially wish to thank the College of Medicine and Pharmacy Research Centers and Deanship of Scientific Research, King Saud University, Riyadh, for funding this work.

Author details

¹Camel Biomedical Research Unit, College of Pharmacy and Medicine, King Saud University, Riyadh, Kingdom of Saudi Arabia. ²Department of Microbiology, South Campus, University of Delhi, New Delhi, India. ³Bioinformatic Centre, North-Eastern Hill University, 793022 Shillong, India. ⁴Laser Applications and Holography Laboratory, Instrument Design Development Centre, Indian Institute of Technology Delhi, 110016 New Delhi, India. ⁵Department of Physiology, College of Medicine, King Saud University, Riyadh, Saudi Arabia.

Received: 15 May 2013 Accepted: 19 July 2013

Published: 29 July 2013

References

1. Carmeliet P, Jain RK: Molecular mechanisms and clinical applications of angiogenesis. *Nature* 2011, **473**:298–307.
2. Eikesdal HP, Sugimoto H, Birrane G, Maeshima Y, Cooke VG, Kieran M, Kalluri R: Identification of amino acids essential for the antiangiogenic activity of tumstatin and its use in combination antitumor activity. *Proc Natl Acad Sci USA* 2008, **105**:15040–15045.
3. Ferrara N: Vascular endothelial growth factor as a target for anticancer therapy. *Oncologist* 2004, **9**:2–10.
4. Ferrara N: VEGF and the quest for tumor angiogenesis factors. *Nat Rev Cancer* 2002, **2**:795–803.
5. Schlessinger J: New roles for Src kinases in control of cell survival and angiogenesis. *Cell* 2000, **100**:293–296.
6. Qi JH, Claesson-Welsh L: VEGF-induced activation of phosphoinositide 3-kinase is dependent on focal adhesion kinase. *Exp Cell Res* 2001, **263**:173–182.
7. Cho CH, Lee CS, Chang M, Jang IH, Kim SJ, Hwang I, Ryu SH, Lee CO, Koh GY: Localization of VEGFR-2 and PLD2 in endothelial caveolae is involved in VEGF-induced phosphorylation of MEK and ERK. *Am J Physiol Heart Circ Physiol* 2004, **286**:H1881–H1888.
8. Kim BW, Choi M, Kim YS, Park H, Lee HR, Yun CO, Kim EJ, Choi JS, Kim S, Rhim H, Kaang BK, Son H: Vascular endothelial growth factor (VEGF) signaling regulates hippocampal neurons by elevation of intracellular calcium and activation of calcium/calmodulin protein kinase II and mammalian target of rapamycin. *Cell Signal* 2008, **20**:714–725.
9. Mao WF, Shao MH, Gao PT, Ma J, Li HJ, Li GL, Han BH, Yuan CG: The important roles of RET, VEGFR2 and the RAF/MEK/ERK pathway in cancer treatment with sorafenib. *Acta Pharmacol Sin* 2012, **33**:1311–1318.
10. Tortora G, Melisi D, Ciardiello F: Angiogenesis: a target for cancer therapy. *Curr Pharm Des* 2004, **10**:11–26.
11. Hoeben A, Landuyt B, Highley MS, Wildiers H, Van Oosterom AT, De Bruijn EA: Vascular endothelial growth factor and angiogenesis. *Pharmacol Rev* 2004, **56**:549–580.
12. Ferrara N, Gerber HP, LeCouter J: The biology of VEGF and its receptors. *Nat Med* 2003, **9**:669–676.
13. Guo S, Colbert LS, Fuller M, Zhang Y, Gonzalez-Perez RR: Vascular endothelial growth factor receptor-2 in breast cancer. *Biochem Biophys Acta* 1806, **2010**:108–121.
14. Niu G, Chen X: Vascular endothelial growth factor as an anti-angiogenic target for cancer therapy. *Curr Drug Targets* 2010, **11**:1000–1017.
15. Holash J, Davis S, Papadopoulos N, Croll SD, Ho L, Russell M, et al: VEGF-Trap: a VEGF blocker with potent antitumor effects. *Proc Natl Acad Sci USA* 2002, **99**:11393–11398.
16. Noble ME, Endicott JA, Johnson LN: Protein kinase inhibitors: insights into drug design from structure. *Science* 2004, **303**:1800–1805.
17. Kamba TT, McDonald DM: Mechanisms of adverse effects of anti-VEGF therapy for cancer. *Br J Cancer* 2007, **96**:1788–1795.
18. Gellert E: In *Alkaloids: Chemical and Biological Perspectives*. Edited by Pelletier SW. New York: Academic Press; 1987:55–132.
19. Gopalakrishnan C, Shankaranarayanan D, Nazimudeen SK, Kameswaran L: Effect of tylophorine, a major alkaloid of *Tylophora indica*, on immunopathological and inflammatory reactions. *Indian J Med Res* 1980, **71**:940–948.
20. Donaldson GR, Atkinson MR, Murray AW: Inhibition of protein synthesis in Ehrlich ascites-tumor cells by the phenanthrene alkaloids tylophorine, tylocrebrine and cryptopleurine. *Biochem Biophys Res Comm* 1968, **31**:104–109.
21. Staerk D, Christensen J, Lemmich E, Duus JØ, Olsen CE, Jaroszewski JW: Cytotoxic activity of some phenanthroindolizidine N-oxide alkaloids from *Cynanchum vincetoxicum*. *J Nat Prod* 2000, **63**:1584–1586.
22. Staerk D, Lykkeberg AK, Christensen J, Budnik BA, Abe F, Jaroszewski JW: In vitro Cytotoxic activity of phenanthroindolizidine alkaloids from *Cynanchum vincetoxicum* and *Tylophora tanakae* against drug-sensitive and multidrug-resistant cancer cells. *J Nat Prod* 2002, **65**:1299–1302.
23. Shiah HS, Gao W, Baker DC, Cheng YC: Inhibition of cell growth and nuclear factor-kb activity in pancreatic cancer cell lines by a tylophorine analogue, DCB-3503. *Mol Cancer Ther* 2006, **5**:2484–2493.
24. Fu Y, Lee SK, Min HY, Lee T, Lee J, Cheng M, Kim S: Synthesis and structure-activity studies of antifolate analogues as potential anticancer agents. *Bioorg Med Chem Lett* 2007, **17**:97–100.
25. Gopalakrishnan C, Shankaranarayanan D, Kameswaran L, Natarajan S: Pharmacological investigations of tylophorine, the major alkaloid of *Tylophora indica*. *Indian J Med Res* 1979, **69**:513–520.
26. Bhutani KK, Sharma GL, Ali M: Plant Based Antiamoebic Drugs; Part I Antiamoebic activity of phenanthroindolizidine alkaloids; common structural determinants of activity with emetine. *Planta Med* 1987, **53**:532–536.
27. Xi Z, Zhang R, Yu Z, Ouyang D: The interaction between tylophorine B and TMV RNA. *Bioorg Med Chem Lett* 2006, **16**:4300–4304.
28. Rao KN, Venkatachalam SR: Inhibition of dihydrofolate reductase and cell growth activity by the phenanthroindolizidine alkaloids pergularinine and tylophorinidine: the in vitro cytotoxicity of these plant alkaloids and their potential as antimicrobial and anticancer agents. *Toxicol In Vitro* 2000, **14**:53–59.
29. Rao KN, Bhattacharya RK, Venkatachalam SR: Inhibition of thymidylate synthase and cell growth by the phenanthroindolizidine alkaloids pergularinine and tylophorinidine. *Chem Biol Interact* 1997, **106**:201–212.
30. Gao W, Lam W, Zhong S, Kaczmarek C, Baker DC, Cheng YC: Novel mode of action of tylophorine analogs as antitumor compounds. *Cancer Res* 2004, **64**:678–688.

31. Gao W, Busson S, Grill SP, Gullen EA, Hu YC, Huang X, Zhong S, Kaczmarek C, Gutierrez J, Francis S, Baker DC, Yu S, et al: **Structure-activity studies of phenanthroindolizidine alkaloids as potential antitumor agents.** *Bioorg Med Chem Lett* 2007, **17**:4338–4342.
32. Wu CM, Yang CW, Lee YZ, Chaung TH, Wu PL, Chao YS, Lee SJ: **Tylophorine arrests carcinoma cells at G1 phase by downregulating cyclin A2 expression.** *Biochem Biophys Res Commun* 2009, **386**:140–145.
33. Shibuya M: **Vascular endothelial growth factor (VEGF)-receptor2: its biological functions, major signaling pathway, and specific ligand VEGF-E.** *Endothelium* 2006, **13**:63–69.
34. Patan S: **Vasculogenesis and angiogenesis.** *Cancer Treat Res* 2004, **117**:3–32.
35. Fong TA, Shawver LK, Sun L, Tang C, App H, Powell TJ, Kim YH, Schreck R, Wang X, Risau W, Ullrich A, Hirth KP, et al: **SU5416 is a potent and selective inhibitor of the vascular endothelial growth factor receptor (Flk-1/KDR) that inhibits tyrosine kinase catalysis, tumor vascularization, and growth of multiple tumor types.** *Cancer Res* 1999, **59**:99–106.
36. Edirisinghe I, Yang SR, Yao H, Rajendrasozhan S, Caito S, Adenuga D, Wong C, Rahman A, Phipps RP, Jin ZG, Rahman I: **VEGFR2 inhibition augments cigarette smoke-induced oxidative stress and inflammatory responses leading to endothelial dysfunction.** *FASEB J* 2008, **22**:2297–2310.
37. Olsson AK, Dimberg A, Kreuger J, Claesson-Welsh L: **VEGF receptor signalling - in control of vascular function.** *Nat Rev Mol Cell Biol* 2006, **7**:359–371.
38. Gerber HP, McMurtrey A, Kowalski J, Yan M, Keyt BA, Dixit V, Ferrara N: **Vascular endothelial growth factor regulates endothelial cell survival through the phosphatidylinositol 3'-kinase/Akt signal transduction pathway, requirement for Flk-1/KDR activation.** *J Biol Chem* 1998, **273**:30336–30343.
39. García-Maceira P, Mateo J: **Silibinin inhibits hypoxia-inducible factor-1 α and mTOR/p70S6K/4E-BP1 signaling pathway in human cervical and hepatoma cancer cells: implications for anticancer therapy.** *Oncogene* 2009, **28**:313–324.
40. Parenti A, Morbidelli L, Cui XL, Douglas JG, Hood JD, Granger HJ, Ledda F, Ziche M: **Nitric oxide is an upstream signal of vascular endothelial growth factor-induced extracellular signal-regulated kinase1/2 activation in postcapillary endothelium.** *J Biol Chem* 1998, **273**:4220–4226.
41. Pober JS, Sessa WC: **Evolving functions of endothelial cells in inflammation.** *Nat Rev* 2007, **7**:803–815.
42. Hlatky L, Hahnfeldt P, Folkman J: **Clinical application of antiangiogenic therapy: microvessel density, what it does and doesn't tell us.** *J Natl Cancer Inst* 2002, **94**:883–893.
43. Chou MT, Wang J, Fujita DJ: **Src kinase becomes preferentially associated with the VEGFR, KDR/Flk-1, following VEGF stimulation of vascular endothelial cells.** *BMC Biochem* 2002, **3**:32.
44. Ali N, Yoshizumi M, Fujita Y, Izawa Y, Kanematsu Y, Ishizawa K, Tsuchiya K, Yano S, Sone S, Tamaki T: **A novel Src kinase inhibitor, M475271, inhibits VEGF-induced human umbilical vein endothelial cell proliferation and migration.** *J Pharmacol Sci* 2005, **98**:130–141.
45. Mitra SK, Schlaepfer DD: **Integrin-regulated FAK-Src signaling in normal and cancer cells.** *Curr Opin Cell Biol* 2006, **18**:516–523.
46. Zachary I, Gliki G: **Signaling transduction mechanisms mediating biological actions of the vascular endothelial growth factor family.** *Cardiovasc Res* 2001, **49**:568–581.
47. Steelman LS, Chappell WH, Abrams SL, Kempf RC, Long J, Laidler P, Mijatovic S, Maksimovic-Ivanic D, Stivala F, Mazzarino MC, Donia M, Fagone P, et al: **Roles of the Raf/MEK/ERK and PI3K/PTEN/Akt/mTOR pathways in controlling growth and sensitivity to therapy-implications for cancer and aging.** *Aging (Albany NY)* 2011, **3**:192–222.
48. Matsuo M, Yamada S, Koizumi K, Sakurai H, Saiki I: **Tumour-derived fibroblast growth factor-2 exerts lymphangiogenic effects through Akt/mTOR/p70S6kinase pathway in rat lymphatic endothelial cells.** *Eur J Cancer* 2007, **43**:1748–1754.
49. Li W, Tan DF, Zhang ZP, Liang JJ, Brown RE: **Activation of Akt-mTOR-p70S6K pathway in angiogenesis in hepatocellular carcinoma.** *Oncol Rep* 2008, **20**:713–719.
50. Fischer C, Mazzone M, Jonck B, Carmeliet P: **FLT1 and its ligands VEGFB and PlGF: drug targets for anti-angiogenic therapy?** *Nat Rev Cancer* 2008, **8**:942–956.
51. Rahimi N: **VEGFR-1 and VEGFR-2: two non-identical twins with a unique physiognomy.** *Front Biosci* 2006, **11**:818–829.
52. Bergers G, Brekken R, McMahon G, Vu TH, Itoh T, Tamaki K, Tanzawa K, Thorpe P, Itohara S, Werb Z, Hanahan D: **Matrix metalloproteinase-9 triggers the angiogenic switch during carcinogenesis.** *Nat Cell Biol* 2000, **2**:737–744.
53. Colavitti R, Pani G, Bedogni B, Anzevino R, Borrello S, Waltenberger J, Galeotti T: **Reactive oxygen species as downstream mediators of angiogenic signaling by vascular endothelial growth factor receptor-2/KDR.** *J Biol Chem* 2002, **277**:3101–3108.
54. Agrawal SS, Saraswati S, Mathur R, Pandey M: **Cytotoxic and antitumor effects of brucine on Ehrlich ascites tumor and human cancer cell line.** *Life Sci* 2011, **89**:147–158.
55. Lee SJ, Lee HM, Ji ST, Lee SR, Mar W, Gho YS: **1,2,3,4,6-Penta-Ogalloyl- β -D-glucose blocks endothelial cell growth and tube formation through inhibition of VEGF binding to VEGF receptor.** *Cancer Lett* 2004, **208**:89–94.
56. Pang X, Yi Z, Zhang X, Sung B, Qu W, Lian X, Aggarwal BB, Liu M: **Acetyl-11-keto- β -boswellic acid inhibits prostate tumor growth by suppressing vascular endothelial growth factor receptor 2-mediated angiogenesis.** *Cancer Res* 2009, **69**:5893–5900.
57. Saraswati S, Pandey M, Mathur R, Agrawal SS: **Boswellic acid inhibits inflammatory angiogenesis in a murine sponge model.** *Microvasc Res* 2011, **82**:263–268.
58. Saraswati S, Agrawal SS: **Strychnine inhibits inflammatory angiogenesis in mice via down regulation of VEGF, TNF- α and TGF- β .** *Microvasc Res* 2013, **87**:7–13.
59. Drabkin DL, Austin JM: **Spectrophotometric constants for common hemoglobin derivatives in human, dog and rabbit blood.** *J Biol Chem* 1932, **98**:719–733.
60. Agrawal SS, Saraswati S, Mathur R, Pandey M: **Antitumor properties of Boswellic acid against Ehrlich ascites cells bearing mouse.** *Food Chem Toxicol* 2011, **49**:1924–1934.
61. Saraswati S, Agrawal SS: **Brucine, an indole alkaloid from Strychnos nuxvomica attenuates VEGF-induced angiogenesis via inhibiting VEGFR2 signaling pathway in vitro and in vivo.** *Cancer Lett* 2013, **332**:83–93.
62. Trott O, Olson AJ: **AutoDock Vina: improving the speed and accuracy of docking with a new scoring function, efficient optimization and multithreading.** *J Computational Chem* 2010, **31**:455–461.
63. Gasteiger J, Marsili M: **Iterative partial equalization of orbital electronegativity-A rapid access to atomic charges.** *Tetrahedron* 1980, **36**:3219–3228.
64. Wallace AC, Laskowski RA, Thornton JM: **LIGPLOT: a program to generate schematic diagram of protein ligand interactions.** *Protein Eng* 1995, **8**:127–134.

doi:10.1186/1476-4598-12-82

Cite this article as: Saraswati et al.: Tylophorine, a phenanthroindolizidine alkaloid isolated from *Tylophora indica* exerts antiangiogenic and antitumor activity by targeting vascular endothelial growth factor receptor 2-mediated angiogenesis. *Molecular Cancer* 2013 **12**:82.

Submit your next manuscript to BioMed Central and take full advantage of:

- Convenient online submission
- Thorough peer review
- No space constraints or color figure charges
- Immediate publication on acceptance
- Inclusion in PubMed, CAS, Scopus and Google Scholar
- Research which is freely available for redistribution

Submit your manuscript at
www.biomedcentral.com/submit

